Designing substrates for silicene and germanene: First-principles calculations

M. X. Chen, Z. Zhong, and M. Weinert

Phys. Rev. B **94**, 075409 — Published 8 August 2016

DOI: 10.1103/PhysRevB.94.075409

Designing substrates for silicene and germanene

M. X. Chen* and M. Weinert
Department of Physics, University of Wisconsin, Milwaukee, Wisconsin 53211, USA

Z. Zhong
Max-Planck-Institute for solid state research, Heisenbergstrasse 1, 70569 Stuttgart, Germany
(Dated: July 13, 2016)

We propose a guideline for exploring substrates that stabilize the monolayer honeycomb structure of silicene and germanene while simultaneously preserve the Dirac states: in addition to have a strong binding energy to the monolayer, a suitable substrate should be a large-gap semiconductor with a proper workfunction such that the Dirac point lies in the gap and far from the substrate states when their bands align. We illustrate our idea by performing first-principles calculations for silicene and germanene on the Al-terminated (0001) surface of Al_2O_3. The overlaid monolayers on Al-terminated Al_2O_3(0001) retain the main structural profile of the low-buckled honeycomb structure via a binding energy comparable to the one between silicene and Ag(111). Unfolded band structure derived from the k-projection method reveals that gapped Dirac cone is formed at the K point due to the structural distortion and the interaction with the substrate. The gaps of 0.4 eV and 0.3 eV respectively for the supported silicene and germanene suggest that they may have potential applications in nanoelectronics.

PACS numbers: 71.20.-b,73.20.-r,73.22.Pr

Silicene, germanene and stanene have attracted considerable attention in recent years since the discovery of graphene for they can host a variety of novel physical phenomena, such as quantum spin Hall effect[1–4], quantum anomalous Hall effect[5–8] and valley Hall effect[9,10], which are related to the Dirac electrons in these unique two-dimensional systems. Moreover, they potentially exhibit extraordinary electronic properties[11–13], holding significant promise for nanoelectronic devices.

However, in sharp contrast to graphene which can be mechanically exfoliated from graphite silicene, germanene and stanene have to be grown on substrates. Up to now, silicene monolayers and multi-layers have been obtained by molecular-beam epitaxial (MBE) growth on Ag(111)[14–23], Ir(111)[24], and ZrB_2(0001)[25]. These systems exhibit a variety of structural reconstructions such as (4×4)[15], $(\sqrt{12}\times\sqrt{12})$, $(\sqrt{13}\times\sqrt{13})$ with respect to the unit cell of Ag(111) and $(\sqrt{3}\times\sqrt{3})$[16] with respect to the 1 × 1 silicene. Most recently, germanene[26–28] and stanene[29] were also obtained by MBE growth. However, the structural reconstruction and the strong hybridization between the grown monolayers and the substrates may significantly modify the electronic structures of the overlayers[20,30–35]. Although theoretical calculations indicate that the Dirac states in the monolayers can be well preserved when they interact with the substrate via vdW-type interactions[31,36–42], the weak layer interactions are unfavorable for stabilizing the low-buckled honeycomb structure. On the other band, it is predicted that the monolayer structure can be stabilized on semiconducting surfaces such as the (111) surface of GaP, GaAs, ZnS, and ZnSe[43,44]. However, electronic bands lose features of the Dirac states. Therefore, it is essentially important to explore substrates that stabilize the monolayer honeycomb structure while simultaneously preserve the Dirac states in the silicene/germanene monolayer.

we propose that a suitable substrate for silicene and germanene should satisfy the following criteria: (i) it has a strong binding energy to the monolayer; (ii) it has a large energy gap; (iii) it has a proper workfunction such that the Dirac point of the monolayer lies in the gap and far from the substrate states when their bands align. We illustrate our idea by performing first-principles calculations for silicene and germanene on the Al-terminated (0001) surface of Al_2O_3. Despite the binding energy between the monolayer structure and Al_2O_3 comparable to that for metal-supported systems, unfolded bands reveal that the Dirac states in silicene and germanene are basically preserved on Al-terminated Al_2O_3(0001). The structural distortion along with the interaction from the substrate induce a gap opening at K, which makes them promising for potential applications in nanoelectronic devices. Moreover, our results reveal that the interaction from the substrate gives rise to minigaps in the band structure of the overlaid monolayers, which will lead to Fermi velocity renormalization and thus affect the electronic transistor properties.

Our concept is illustrated in Fig. 1. When a substrate and a monolayer with Dirac states are brought to interact, their bands are aligned according to that their vacuum levels are aligned the same. The interaction of between them is denoted by V_{int}. Similar to the heteronuclear diatomic systems the resulting perturbations to the electronic bands of the isolated systems are determined by both the interaction and the difference (ΔE) in the energy levels between the two constituents. Strong perturbations to the Dirac states can be expected when V_{int} is large and ΔE is small. In particular, the silicene/germanene bands are strongly destroyed when it is placed onto metal substrates because of the strong layer

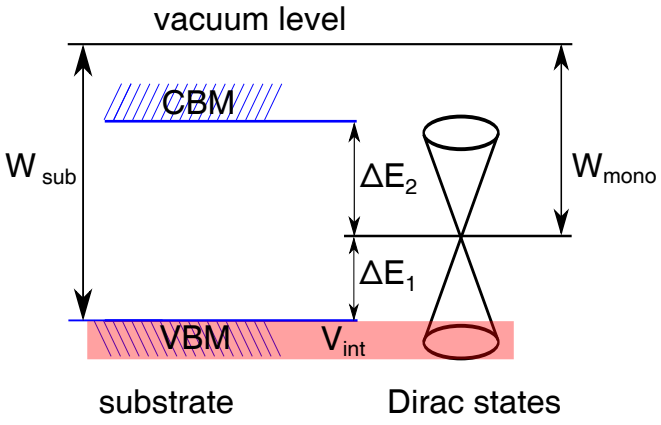

FIG. 1. Schematic illustration of the interaction between a semiconducting substrate and a monolayer with Dirac states. W_{sub} (W_{mono}) represents the workfunction of the substrate (the monolayer). ΔE_i denote the energy differences between the substrate states and the Dirac point. V_{int} stands for the interaction between the substrate and the monolayer. VBM and CBM represent the valence band maximum and conduction band minimum, respectively.

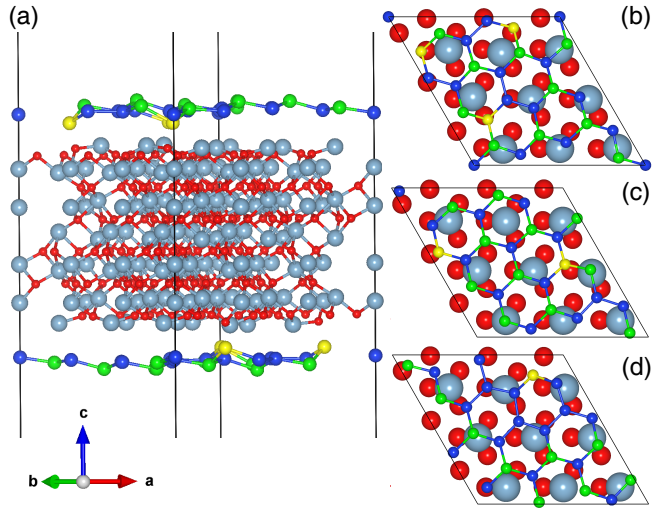

FIG. 2. Structure of ($\sqrt{13} \times \sqrt{13}$) silicene on (3×3) Al-terminated Al_2O_3(0001). (a) Perspective view and (b) top view of the relaxed S1 structure. Top view of the relaxed (c) S2 and (d) S3 structures. Si atoms are represented by blue, green (buckling away from the substrate), and yellow (buckling towards) balls.

interaction and that ΔE is zero. Whereas, the Dirac states can be preserved well in vdW heterostructures since V_{int} is small. However, to stabilize the monolayer honeycomb structure a strong binding between silicene (germanene) and the substrate is required, that is, V_{int} is large. Therefore, to avoid a strong disturbance to the Dirac states ΔE should be large, that is, the Dirac states should be far from the substrate states. For such a purpose, large-gap semiconductors with a proper workfunction are desirable such that the Dirac states lie in the middle of the gap when their bands align. Of course, the interaction with the substrate may affect the structure and correspondingly modifies the electronic bands of the overlayer.

As a large-gap semiconductor, Al_2O_3 has been widely used as a substrate in silicon-based semiconducting devices. A simple density-functional theory (DFT) calculation indicates that Al-terminated Al_2O_3(0001) is a semiconductor with a gap about 4.84 eV and a work function of about 6.60 eV. While the ideal low-buckled silicene has a workfunction of about 4.76 eV. By the band alignment, one can find that the Dirac cone of the silicene lies in the gap of Al-terminated Al_2O_3(0001), and is 1.94 ev and 2.90 eV from the VBM and CBM, respectively. Such energy separations imply that the Dirac states in silicene may experience a relatively weak perturbation (compared to silicene/Ag(111)) even though the monolayer has a strong binding with the substrate as well.

To validate our ideal, we performed DFT calculations for silicene on Al_2O_3(0001) using the Vienna Ab initio Simulation Package[45,46]. The pseudopotentials were constructed by the projector augmented wave method[47,48]. Van der Waals dispersion forces between the adsorbate and the substrate were accounted for through the optPBE-vdW functional by using the vdW-DF method developed by Klimeš and Michaelides[49,50]. A 4×4 Monkhorst-Pack k-mesh was used to sample the surface BZ and a plane-wave energy cut off of 400 eV was used for structural relaxation and electronic structure calculations.

In our calculations the substrate Al_2O_3(0001) was modeled by a slab consisting of 6 Al_2O_3 layers (12 Al and six oxygen layers), with the two surfaces terminated by Al-I since this termination was found to be more stable than the Al-II and the O-terminated surfaces[51]. Because the spacing between the top Al layer and the next O layer is significantly reduced upon structural relaxation[51], the slab was firstly fully relaxed. Then a ($\sqrt{13} \times \sqrt{13}$) silicene layer is placed on each side of a (3×3) supercell of Al_2O_3(0001), which gives rise to a small lattice mismatch (∼2.8%). The silicene/Al_2O_3(0001) slab is separated from its periodic images by ∼20 Åvacuum regions. For the structural relaxation of silicene/Al_2O_3(0001) the Si atoms and the top Al and O atoms were allowed to relax, with a threshold of 0.001 eV/Å for the residual force on each atom, while the positions of the other atoms were frozen.

Three types of configurations are considered for silicene/Al_2O_3(0001) as shown in Fig. 2, which are denoted by S1, S2, and S3, respectively. S2 (S3) has a Si atom at a top site over Al (O), whereas in S1 none of Si atoms is exactly sitting on a top site. S1 is energetically more favorable than S2 and S3 by 0.023 eV/Si and 0.024 eV/Si, respectively. Our calculations indicate that silicene - substrate distance is increased by about 0.28 Å when vdW correction is taken into account. The relaxed structures of silicene are buckled similarly to ideal

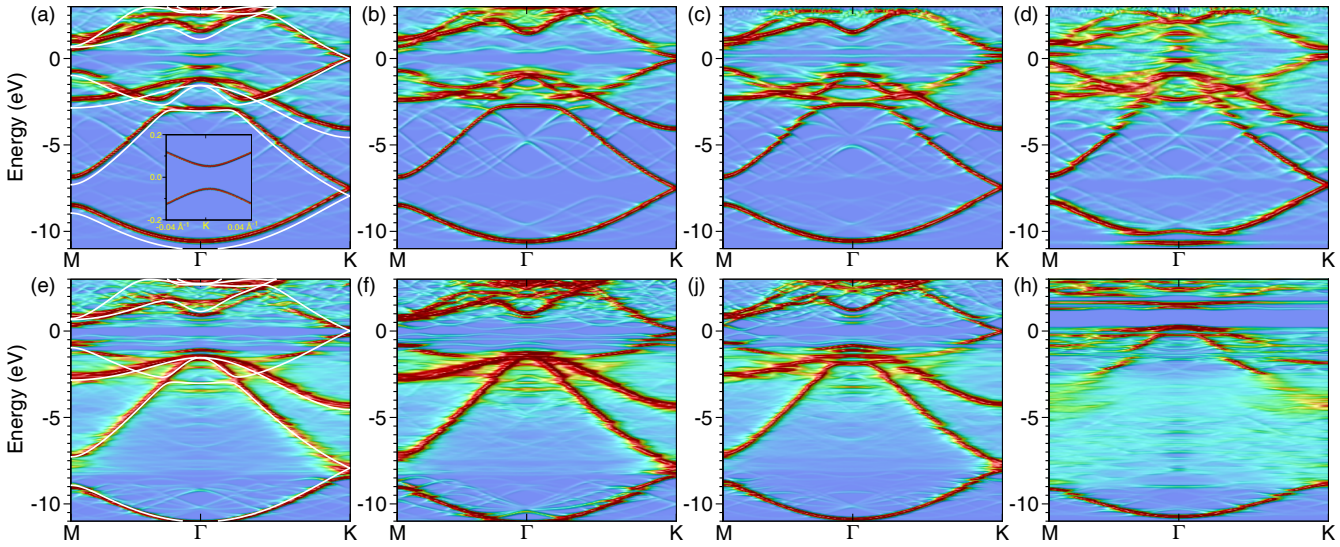

FIG. 3. Electronic bands of silicene. (a)-(c) k-projected bands in the (1×1) BZ for isolated silicene in the S1, S2, and S3 structures, respectively; (e)-(j) the corresponding bands for supported silicene on Al-terminated $Al_2O_3(0001)$. (d) and (h) k-projected bands for isolated and supported silicene on O-terminated $Al_2O_3(0001)$, respectively. Bands of ideal(1×1) silicene are shown as solid white lines overlaid for comparison. The inset in (a) shows bands about K in the range ±0.04 $Å^{-1}$. The Fermi level is set to be zero.

low-buckled silicene, but with significant deviations from the alternating buckling pattern of ideal silicene caused by interactions with the substrate. For S1 the large downward bucklings are about 0.9 Å, which reduces the layer distance down to about 1.4 Å. Together with the low-buckled Si atoms, this gives rise to a thickness of about 1.5 Åfor the silicene. Si-Si bond lengths for the relaxed structures are between 2.30 and 2.42 Å, comparable to those of ideal silicene (2.30 Å). The binding energy of 0.52 eV/Si is comparable to 0.698 eV/Si for silicene/Ag(111)[31] but much higher than that for silicene/graphene (∼ 0.1 eV/Si), favoring stabilizing the monolayer structure.

The coexistence of low- and high-buckling in the supported silicene results in a reconstructed structure which no longer has the (1×1) silicene periodicity, but still maintains the basic honeycomb structure. Therefore, the bands can still be unfolded into the (1×1) silicene BZ by projecting the supercell wave functions onto the corresponding k of the (1×1) silicene cell[30,52], i.e., the structural distortion/reconstruction serves as a perturbation to the (1×1) silicene bands.

Figures. 3(a)-(c) show the k-projected bands for isolated silicene corresponding to the three configurations shown in Figs. 2(b)-(d), respectively, with the bands of the ideal silicene shown for comparison. The isolated (reconstructed) silicene bands basically preserve the main feature of the ideal structure, although there are distinct differences. The most prominent one is the opening of a gap at the Dirac point at K due to the symmetry breaking caused by the structural reconstruction. The size of the gap varies for the different structures, and is about 0.1 eV for the lowest energy structure S1. Moreover, the reconstruction gives rise to minigaps in the linear dispersion around K, and slightly renormalizes the band widths compared to those of the ideal structure, c.f., Fig. 3(a).

Although the band structures for silicene are basically preserved upon supported by Al-terminated $Al_2O_3(0001)$ the effect of the substrate for supported silicene, Figs. 3(e)-(j), are noticeable around the Fermi energy: The gap at K for the lowest energy S1 structure is enhanced to 0.44 eV; additional minigaps are introduced (due to the different substrate periodicity); and (comparing Figs. 3(a) and (e)) the substrate induces a shift of the silicene bands of about 0.5 eV relative to the Fermi level. Whereas a comparison of Figs. 3(d) and (h) shows that silicene bands are significantly disturbed by O-terminated $Al_2O_3(0001)$. In particular, the bands near the Fermi level lose features of gapped Dirac cone near K as obtained for the isolated silicene.

The band structure of silicene on $Al_2O_3(0001)$ shows also distinct differences from metal-supported silicene[20,30–35] and silicene-based vdW heterostructures[31,36–42]. In the former case, the silicene bands are strongly hybridized with those of the substrate so that the bands at the K point are significantly destroyed, no longer having Dirac-electron character, while the linear dispersions are well preserved in silicene-based vdW heterostructures. Moreover, the binding between silicene and Al-terminated $Al_2O_3(0001)$ together with the structural and electronic properties of the supported silicene may somehow support that silicene can be properly stabilized by a Al_2O_3 encapsulation layer[53], although the encapsulation layer is likely amorphous in the experiment.

To gain further insights into the interaction between

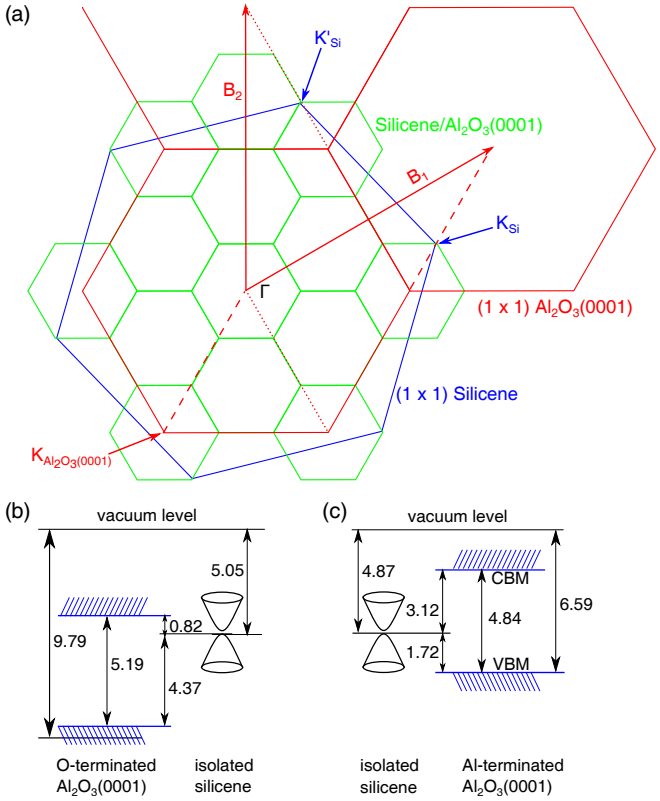

FIG. 4. Interaction between silicene and $Al_2O_3(0001)$. (a) BZs of silicene/$Al_2O_3(0001)$, (1×1) silicene and $Al_2O_3(0001)$ shown in green, blue and red, respectively. $\mathbf{B_1}$ and $\mathbf{B_2}$ represent the reciprocal lattice vectors of (1×1) $Al_2O_3(0001)$. (b), (c) Band alignment of the isolated silicene and O-terminated and Al-terminated (0001) surfaces of Al_2O_3, respectively. In the case of Al-terminated $Al_2O_3(0001)$, the isolated systems are obtained from configuration S1. The calculated work functions and the gaps of $Al_2O_3(0001)$ are shown. VBM and CBM represent the valence band maximum and conduction band minimum, respectively.

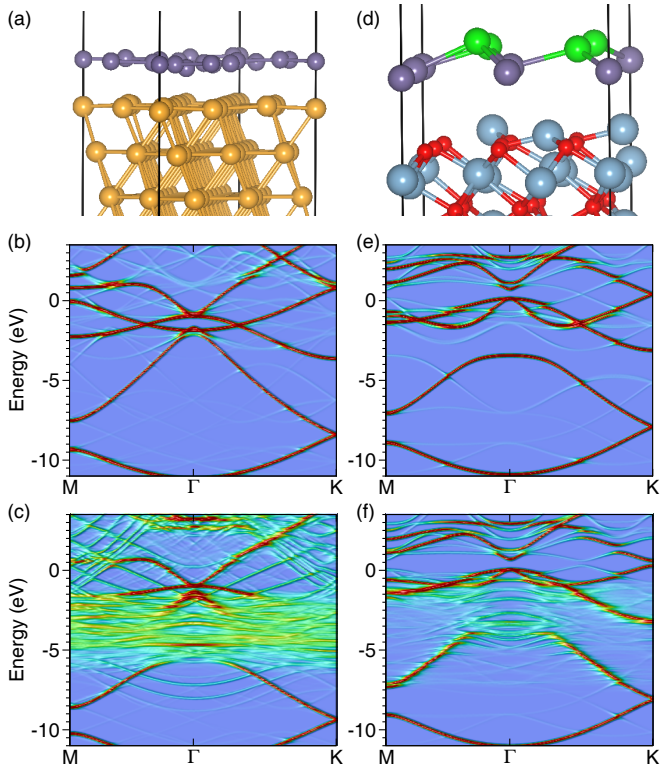

FIG. 5. DFT calculations of germanene on Au(111) and $Al_2O_3(0001)$. (a) Relaxed structure of (3×3) germanene on $(\sqrt{19} \times \sqrt{19})$ Au(111). (b) and (c) k-projected bands for isolated and supported germanene, respectively. (d) - (f) Corresponding results for (2×2) germanene on $(\sqrt{3} \times \sqrt{3})$ $Al_2O_3(0001)$. Buckled Ge atoms are shown in green balls.

the states of silicene and $Al_2O_3(0001)$, Fig. 4(a) shows the supercell BZs of silicene/$Al_2O_3(0001)$, and the BZs of the ideal silicene and the substrate. Note that the $2/3\mathrm{K}_{\mathrm{Al_2O_3}}$ ($\mathrm{K'_{Al_2O_3}}$) coincides with $\mathrm{K_{Si}}$ ($\mathrm{K'_{Si}}$) by a translation of a reciprocal lattice vector of (1×1) $Al_2O_3(0001)$, $\mathbf{B_1}$ ($\mathbf{B_2}$). When silicene is overlaid onto $Al_2O_3(0001)$, the wavefunctions of silicene Ψ_{Si} (K_{Si}) interact with those of $Al_2O_3(0001)$ $\Psi_{\mathrm{Al_2O_3}}$ ($\frac{2}{3}$ $K_{\mathrm{Al_2O_3}}$+$\mathbf{B_1}$). Figs. 4(b) and (c) shows the band alignment of the two constituents before interacting. In the case of silicene/O-terminated-$Al_2O_3(0001)$ the gapped Dirac states of silicene are close to the conduction band of the substrate. This along with the strong interaction between them (E_b is larger than 1.0 eV) lead to strong modifications over the silicene bands. Whereas, for silicene/Al-terminated-$Al_2O_3(0001)$ (configuration S1) the Dirac states of silicene are in the gap of the substrate, far from the substrate states. Therefore despite the strong binding between the two constituents, there is little direct bonding of between the silicene Dirac states and the Al_2O_3 states. By projecting the wavefunctions over atomic orbitals, we find that Si-pz orbitals contribute over 75% to the VBM and CBM. Whereas, the substrate just has little contributions.

Likewise, a DFT calculation shows that the work function of an ideal low-buckled germanene is about 4.66 eV, which will place the Dirac point in the gap of Al-terminated $Al_2O_3(0001)$ according to the band alignment and will gives rise to an energy separation of about 1.93 (2.91) eV between the Dirac point and the VBM (CBM) of the substrate, respectively. Therefore, one may expect that the Dirac states are likely preserved when the germanene monolayer is overlaid onto Al-terminated $Al_2O_3(0001)$. DFT calculations were then performed for germanene on Al-terminated $Al_2O_3(0001)$, of which the k-projected bands are shown in Fig. 5. The band structures for germanene on Au(111) are also shown for comparison. The relaxed structure of germanene on Au(111) is pretty much similar to the planar hexagonal structure. Therefore, the k-projected bands for the isolated germanene are in great similarity to those for the planar germanene[54]. However, its electronic bands experience dramatic changes when germanene is placed on Au(111). From Fig. 5(c) one can see that germanene-derived bands in the energy window of -6.0 eV - 3.0 eV are strongly de-

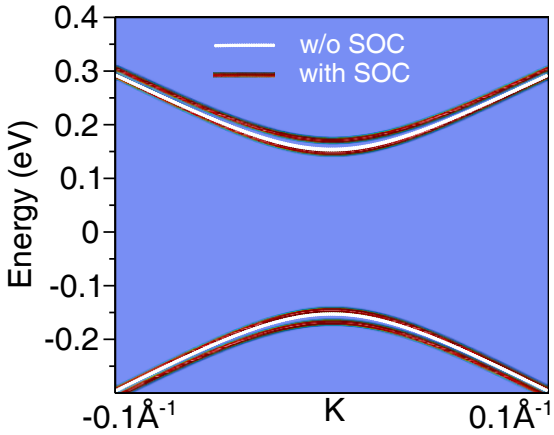

FIG. 6. Band structure with SOC about the K point for germanene/Al_2O_3(0001). The bands without SOC (in white) are overlaid for comparison.

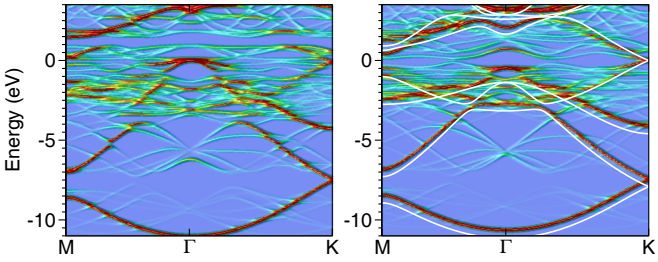

FIG. 7. k-projected bands for isolated silicene in the structure calculated for (a) ($\sqrt{12} \times \sqrt{12}$) and (b) ($\sqrt{13} \times \sqrt{13}$) Ag(111). Bands for ideal silicene are shown as white lines for comparison.

stroyed. In particular, near the Fermi level the linear dispersions at the K point become indistinguishable. This is due to the strong hybridization between the substrate bands and the Dirac states. However, germanene on Al_2O_3 exhibits distinct differences. Fig. 5(d) shows that the relaxed structure of supported germanene basically remains the global profile of the ideal low-buckled structure. Therefore it is not surprising that the k-projected band structure for the isolated germanene bears a great similarity to that for the ideal germanene, except for minigaps near $\pm$ 1.0 eV (Fig. 5(e)). Upon the presence of Al-terminated Al_2O_3(0001), the linear dispersions near K are preserved well, except for the minigap near 1.0 eV and the gap at K are slightly enhanced.

It is demonstrated that external electric field can be used to tune the energy gap of silicene[12,13]. Therefore, in addition to band hybridization, electric field induced by the substrate may be responsible for the changes in the band gaps of silicene and germanene upon supported. It should be mentioned that the energy gaps of our systems obtained using the standard DFT may be underestimated. More accurate descriptions can be achieved by using hybrid functionals and GW methods. However, such calculations are not feasible for our systems with a larger number of atoms in the unit cell. Nevertheless, our results indicate that the Al-terminated Al_2O_3(0001) not only stabilizes the monolayer structure of silicene and germanene, but also tunes their energy gap for potential applications in electronic devices.

Spin-orbit coupling (SOC) is important for the predicted quantum spin Hall effect in the ideal low-buckled silicene and germanene, which induces a gap opening at the K point. The SOC gaps are about 1.55 meV and 23.9 meV for silicene and germanene, respectively[1]. Our calculations without including SOC show that gap opening occurs in the presence of the substrate (see Fig. 3 and Fig. 5), which is due to the symmetry breaking in the sublattice. SOC calculations were further performed to investigate the effect of SOC on the band structure of germanene/Al_2O_3(0001). Fig. 6 shows that SOC induces splittings in both the valence and the conduction bands, which are about 25 meV at the K point. Likewise, our calculations (plot not shown) for the case of silicene find that SOC splittings at K are about 1.5 meV.

Our results can shed light on the degradation of carrier mobility observed for silicene-field effect transistors, where silicenes directly contact with Al_2O_3 (although the substrate may be amorphous), that is, the measured electron mobility was an order of magnitude lower than predicted for the ideal silicene[55]. An important issue is that the silicenes investigated in the present study differ from the experimental ones. In Tao's experiments, silicene is either in ($\sqrt{12} \times \sqrt{12}$) or ($\sqrt{13} \times \sqrt{13}$) with respect to the ($1 \times 1$) Ag(111) (which is ($\sqrt{7} \times \sqrt{7}$) with respect to the ($1 \times 1$) silicene). Fig. 7 shows k-projected bands for isolated silicene in the structures corresponding to ($\sqrt{12} \times \sqrt{12}$) and ($\sqrt{13} \times \sqrt{13}$) Ag(111). The folded bands for these structures agree well those reported by previous studies[31,56]. Although Dirac-like bands at K are observed in the folded band structure for the isolated silicene on ($\sqrt{13} \times \sqrt{13}$) Ag(111), k-projected bands indicate that silicene bands undergo considerable changes upon the structural distortion. The effects of the structural reconstruction are much more pronounced for the supported silicene on ($\sqrt{12} \times \sqrt{12}$) Ag(111). For ($\sqrt{7} \times \sqrt{7}$) silicene placed onto Al_2O_3(0001), a supercell of ($\sqrt{21} \times \sqrt{21}$) is required to obtain a small lattice mismatch of $\sim$2%, and a corresponding substrate ($\sqrt{13} \times \sqrt{13}$) supercell. While such calculations might be possible, we have not attempted them; nevertheless, based on the above results one may expect similar effects of the substrate on the ($\sqrt{7} \times \sqrt{7}$) silicene as seen here. Moreover, our calculations are consistent with experiments that a gap is formed in the band structure of silicene on Al_2O_3 (Fig. 3).

The electron mobility is determined by the Fermi velocity and relaxation times of electrons due to various scattering processes, i.e., $\mu = v^2\tau$. Fig. 3 shows that the structural reconstruction renormalizes the electronic bands and therefore renormalizes the Fermi velocity as well. By a comparison of bands for the ideal silicene and the isolated one (Fig. 3(a)), a decrease in the Fermi velocity for the supported silicene is found. Moreover,

the substrate interactions and the silicene reconstruction induce minigaps in the band structure of silicene, which also significantly reduce the Fermi velocity near the minigaps. The structural reconstructions also modify the phonon spectrum of silicene and thus the intrinsic electron-phonon scattering relaxation time. In addition, surface polar phonon of the substrate may play a role in scatterings electrons in the overlayer[57,58], further reducing the electron mobility.

In summary, we propose a guideline for exploring suitable substrates for silicene and germanene. Our DFT calculations find that Al-terminated $Al_2O_3(0001)$ may be a good candidate: although silicene (germanene) experiences structural distortions due to the interaction with the substrate, the main profile of the ideal low-buckled structure is maintained. Unlike the metal-supported monolayers, where Dirac electrons are absent, a gapped Dirac cone is formed at the K point in silicene as well as germanene on Al-terminated $Al_2O_3(0001)$. However, Al_2O_3 as a substrate has substantial effects on the electronic bands of silicene: not only inducing a band gap at the K point, but also giving rise to minigaps in the band structure, which will lead to Fermi velocity renormalization and thus affect the electronic transport properties. Our results not only can shed light on recent transport experiments on silicene-based transistors, but also may aid in the design of silicene/germanene-based electronic devices.

ACKNOWLEDGMENTS

This work was supported by the U.S. Department of Energy, Office of Basic Energy Sciences, Division of Materials and Engineering under Award DE-FG02-07ER46228 and the U.S. National Science Foundation, Division of Materials Research under agreement DMR-1508560.

* chen59@uwm.edu

[1] C.-C. Liu, W. Feng, and Y. Yao, Phys. Rev. Lett. **107**, 076802 (2011).
[2] Y. Xu, B. Yan, H.-J. Zhang, J. Wang, G. Xu, P. Tang, W. Duan, and S.-C. Zhang, Phys. Rev. Lett. **111**, 136804 (2013).
[3] Y. Ma, Y. Dai, C. Niu, and B. Huang, J. Mater. Chem. **22**, 12587 (2012).
[4] L. Seixas, J. E. Padilha, and A. Fazzio, Phys. Rev. B **89**, 195403 (2014).
[5] M. Ezawa, Phys. Rev. Lett. **109**, 055502 (2012).
[6] T. P. Kaloni, J. Phys. Chem. C **118**, 25200 (2014), http://dx.doi.org/10.1021/jp5058644.
[7] T. P. Kaloni, N. Singh, and U. Schwingenschlögl, Phys. Rev. B **89**, 035409 (2014).
[8] S.-M. Huang, S.-T. Lee, and C.-Y. Mou, Phys. Rev. B **89**, 195444 (2014).
[9] M. Ezawa, Phys. Rev. B **87**, 155415 (2013).
[10] C. J. Tabert and E. J. Nicol, Phys. Rev. B **87**, 235426 (2013).
[11] Z. Ni, Q. Liu, K. Tang, J. Zheng, J. Zhou, R. Qin, Z. Gao, D. Yu, and J. Lu, Nano Lett. **12**, 113 (2012).
[12] N. D. Drummond, V. Zlyomi, and V. I. Fal'ko, Phys. Rev. B **85**, 075423 (2012).
[13] M. Ezawa, New J. Phys. **14**, 033003 (2012).
[14] B. Lalmi, H. Oughaddou, H. Enriquez, A. Kara, S. Vizzini, B. Ealet, and B. Aufray, Appl. Phys. Lett. **97**, 2231092 (2010).
[15] P. Vogt, P. De Padova, C. Quaresima, J. Avila, E. Frantzeskakis, M. C. Asensio, A. Resta, B. Ealet, and G. Le Lay, Phys. Rev. Lett. **108**, 155501 (2012).
[16] L. Chen, C.-C. Liu, B. Feng, X. He, P. Cheng, Z. Ding, S. Meng, Y. Yao, and K. Wu, Phys. Rev. Lett. **109**, 056804 (2012).
[17] B. Feng, Z. Ding, S. Meng, Y. Yao, X. He, P. Cheng, L. Chen, and K. Wu, Nano Lett. **12**, 3507 (2012).
[18] R. Arafune, C.-L. Lin, K. Kawahara, N. Tsukahara, E. Minamitani, Y. Kim, N. Takagi, and M. Kawai, Surface Science **608**, 297 (2013).
[19] L. Chen, H. Li, B. Feng, Z. Ding, J. Qiu, P. Cheng, K. Wu, and S. Meng, Phys. Rev. Lett. **110**, 085504 (2013).
[20] C.-L. Lin, R. Arafune, K. Kawahara, M. Kanno, N. Tsukahara, E. Minamitani, Y. Kim, M. Kawai, and N. Takagi, Phys. Rev. Lett. **110**, 076801 (2013).
[21] Z.-L. Liu, M.-X. Wang, J.-P. Xu, J.-F. Ge, G. L. Lay, P. Vogt, D. Qian, C.-L. Gao, C. Liu, and J.-F. Jia, New J. Phys. **16**, 075006 (2014).
[22] P. De Padova, P. Vogt, A. Resta, J. Avila, I. Razado-Colambo, C. Quaresima, C. Ottaviani, B. Olivieri, T. Bruhn, T. Hirahara, T. Shirai, S. Hasegawa, M. Carmen Asensio, and G. Le Lay, Appl. Phys. Lett. **102**, 163106 (2013).
[23] A. J. Mannix, B. Kiraly, B. L. Fisher, M. C. Hersam, and N. P. Guisinger, ACS Nano **8**, 7538 (2014).
[24] L. Meng, Y. Wang, L. Zhang, S. Du, R. Wu, L. Li, Y. Zhang, G. Li, H. Zhou, W. A. Hofer, and H.-J. Gao, Nano Lett. **13**, 685 (2013).
[25] A. Fleurence, R. Friedlein, T. Ozaki, H. Kawai, Y. Wang, and Y. Yamada-Takamura, Phys. Rev. Lett. **108**, 245501 (2012).
[26] L. Li, S.-Z. Lu, J. Pan, Z. Qin, Y.-Q. Wang, Y. Wang, G.-Y. Cao, S. Du, and H.-J. Gao, Adv. Mater. **26**, 4820 (2014).
[27] M. E. Dvila, L. Xian, S. Cahangirov, A. Rubio, and G. L. Lay, New J. Phys. **16**, 095002 (2014).
[28] M. Derivaz, D. Dentel, R. Stephan, M.-C. Hanf, A. Mehdaoui, P. Sonnet, and C. Pirri, Nano Lett. **15**, 2510 (2015), pMID: 25802988, http://dx.doi.org/10.1021/acs.nanolett.5b00085.
[29] F.-F. Zhu, W.-J. Chen, Y. Xu, C.-L. Gao, D.-D. Guan, C.-H. Liu, D. Qian, S.-C. Zhang, and J.-F. Jia, Nat. Mater. **14**, 1020 (2015).
[30] M. X. Chen and M. Weinert, Nano. Lett. **14**, 5189 (2014).
[31] Z.-X. Guo, S. Furuya, J.-i. Iwata, and A. Oshiyama, Phys. Rev. B **87**, 235435 (2013).
[32] Y.-P. Wang and H.-P. Cheng, Phys. Rev. B **87**, 245430

(2013).
[33] S. Cahangirov, M. Audiffred, P. Tang, A. Iacomino, W. Duan, G. Merino, and A. Rubio, Phys. Rev. B **88**, 035432 (2013).
[34] R. Quhe, Y. Yuan, J. Zheng, Y. Wang, Z. Ni, J. Shi, D. Yu, J. Yang, and J. Lu, Sci. Rep. **4**, 5476 (2014).
[35] S. K. Mahatha, P. Moras, V. Bellini, P. M. Sheverdyaeva, C. Struzzi, L. Petaccia, and C. Carbone, Phys. Rev. B **89**, 201416 (2014).
[36] Y. Cai, C.-P. Chuu, C. M. Wei, and M. Y. Chou, Phys. Rev. B **88**, 245408 (2013).
[37] M. Houssa, G. Pourtois, V. V. Afanasev, and A. Stesmans, Appl. Phys. Lett. **97**, 112106 (2010), http://dx.doi.org/10.1063/1.3489937.
[38] T. P. Kaloni and U. Schwingenschlgl, J. Appl. Phys. **114**, 184307 (2013), http://dx.doi.org/10.1063/1.4830016.
[39] Y. Ding and Y. Wang, Appl. Phys. Lett. **103**, 043114 (2013), http://dx.doi.org/10.1063/1.4816753.
[40] E. Scalise, M. Houssa, E. Cinquanta, C. Grazianetti, B. van den Broek, G. Pourtois, A. Stesmans, M. Fanciulli, and A. Molle, 2D Mat. **1**, 011010 (2014).
[41] S. Kokott, P. Pflugradt, L. Matthes, and F. Bechstedt, J. Phys.: Condens. Matter **26**, 185002 (2014).
[42] N. Gao, J. C. Li, and Q. Jiang, Phys. Chem. Chem. Phys. **16**, 11673 (2014).
[43] A. Bhattacharya, S. Bhattacharya, and G. P. Das, Appl. Phys. Lett. **103**, 123113 (2013), http://dx.doi.org/10.1063/1.4821993.
[44] T. P. Kaloni, G. Schreckenbach, M. S. Freund, and U. Schwingenschlgl, Phys. Status Solidi RRL **10**, 133 (2016).
[45] G. Kresse and J. Furthmüller, Comput. Mater. Sci. **6**, 15 (1996).
[46] G. Kresse and J. Furthmüller, Phys. Rev. B **54**, 11169 (1996).
[47] P. E. Blöchl, Phys. Rev. B **50**, 17953 (1994).
[48] G. Kresse and D. Joubert, Phys. Rev. B **59**, 1758 (1999).
[49] J. Klimeš, D. R. Bowler, and A. Michaelides, Phys. Rev. B **83**, 195131 (2011).
[50] J. Klimeš, D. R. Bowler, and A. Michaelides, J. Phys.: Condens. Matter **22**, 022201 (2010).
[51] T. Kurita, K. Uchida, and A. Oshiyama, Phys. Rev. B **82**, 155319 (2010).
[52] Y. Qi, S. H. Rhim, G. F. Sun, M. Weinert, and L. Li, Phys. Rev. Lett. **105**, 085502 (2010).
[53] A. Molle, C. Grazianetti, D. Chiappe, E. Cinquanta, E. Cianci, G. Tallarida, and M. Fanciulli, Adv. Funct. Mater. **23**, 4340 (2013).
[54] S. Cahangirov, M. Topsakal, E. Akturk, H. Sahin, and S. Ciraci, Phys. Rev. Lett. **102**, 236804 (2009).
[55] L. Tao, E. Cinquanta, D. Chiappe, C. Grazianetti, M. Fanciulli, M. Dubey, A. Molle, and D. Akinwande, Nat. Nano. **10**, 227 (2015).
[56] E. Scalise, E. Cinquanta, M. Houssa, B. van den Broek, D. Chiappe, C. Grazianetti, G. Pourtois, B. Ealet, A. Molle, M. Fanciulli, V. V. Afanasev, and A. Stesmans, Appl. Surf. Sci. **291**, 113 (2014).
[57] S. Fratini and F. Guinea, Phys. Rev. B **77**, 195415 (2008).
[58] J.-H. Chen, C. Jang, S. Xiao, M. Ishigami, and M. S. Fuhrer, Nat. Nano. **3**, 206 (2008).